Gradual Molding of the Hand to Object Contours

MARCO SANTELLO AND JOHN F. SOECHTING
Department of Physiology, University of Minnesota, Minneapolis, Minnesota 55455

Santello, Marco and John F. Soechting. Gradual molding of the hand to object contours. *J. Neurophysiol.* 79: 1307–1320, 1998. Subjects were asked to reach to and to grasp 15 similarly sized objects with the four fingers opposed to the thumb. The objects' contours differed: some presented a concave surface to the fingers, others a flat one, and yet others a convex surface. Flexion/extension at the metacarpal-phalangeal and proximal interphalangeal joints of the fingers was recorded during the reaching movement. We used discriminant analysis, cluster analysis, and information theory to determine the extent to which the shape of the hand was affected by the objects' shapes along a convexity/concavity gradient. Maximum aperture of the hand was reached about midway in the reaching movement. At that time, the hand's posture was influenced by the shape of the object to be grasped but imperfectly. The information transmitted by hand posture about object shape increased gradually and monotonically as the hand approached the object, reaching a maximum at the time the object was in the grasp of the hand. We also asked subjects to shape the hand so as to grasp the object without moving the arm. Their performance was poorer on this task in the sense that hand shape discriminated among fewer objects and that trial-to-trial variability was greater than when the distal and proximal components of the motion were linked. The results indicate that the hand is molded only gradually to the contours of an object to be grasped. Because other parameters of the motion, such as movement direction, for example, already are specified fully early on in a movement, the results also suggest that the specification of diverse aspects of a movement does not evolve at a uniform rate.

INTRODUCTION

As one reaches to grasp an object, the hand's aperture, of necessity, increases to a maximum that exceeds the object's size as the hand approaches it. The maximum aperture between two fingers is known to be related linearly to the object's size (cf. Chieffi and Gentilucci 1993; Jeannerod 1981; Marteniuk et al. 1990; Paulignan et al. 1991). However, there are many other factors that also can be expected to influence the shape of the hand during a grasping movement. Foremost among these is how the object is intended to be used; long ago Napier (1956) showed that hand shape depended on this factor. The shape of an object also can be expected to influence the posture of the hand during a grasping movement. In general, not all potential points of contact of the hand with an object will lead to stable grasps (Cutkosky and Howe 1990). Therefore one also might expect the points of contact to be planned or specified during the transport phase of the movement. If so, the shape of the hand before contact should depend on object shape as well as on object size.

Nevertheless, it is possible that under certain conditions the precise shape of an object could be largely ignored. For example, consider two objects, one convex and the other concave, that have approximately the same size. Assume that both objects are to be grasped by all four fingers in opposition to the thumb. As long as the hand is opened far enough to encompass each of the objects, the precise configuration of each of the fingers need not be specified a priori. Instead, subjects could take advantage of the compliant characteristics of the hand (cf. Hajian and Howe 1997) and use tactile feedback generated by contact of the hand with the object (Johansson and Cole 1992) to mold the hand precisely to the object's contour. Such a strategy could simplify the control of hand posture during grasping because it would minimize the number of hand shapes that would be realizable during the transport phase (Iberall and Fagg 1996; Iberall and MacKenzie 1990).

The experiments to be described in this paper were designed to test this hypothesis. We asked subjects to reach for and to grasp a variety of objects, all having roughly the same size but differing in shape, and we measured the motion of all of the fingers. Contrary to the hypothesis outlined above, we found that the posture of the hand discriminated among the various shapes well before contact with the objects. However, this discrimination was incomplete at the time of peak aperture. Instead, the dependence of hand shape on object shape evolved gradually throughout the movement, suggesting that this parameter is not specified fully at the time of maximum hand opening.

METHODS

Experimental tasks

Subjects were required to grasp 15 different objects the shapes of which ranged from convex to concave (Fig. 1). Each of the objects consisted of a block of plywood, 12 cm in height and 2.4 cm thick, weighing ∼100 g. They were meant to be grasped between the four fingers and the thumb of the right hand, and they were designed to have approximately the same size (i.e., to require similar maximum apertures of the hand). Some of the objects presented a flat face to the fingers (for example *object 1,* Fig. 1). Others were concave (e.g., *objects 2, 4,* and *14*); at contact one would expect the middle and ring fingers to be in a more flexed posture than the index and little fingers. Others were convex (e.g., *objects 8, 10,* and *15*), requiring more flexion at the index and little fingers than at the other two fingers. *Object 12* required more extension at the index finger than at the other fingers, whereas *object 13* (obtained by a rotation of *object 12* about the horizontal axis) required more extension at the little finger. *Objects 6* and *7* presented flat faces that were inclined relative to the vertical, whereas *objects 3, 5, 9,* and *11* (obtained by rotation of the illustrated objects about the vertical axis) all presented flat, vertical faces to the four fingers.

Subjects were instructed to reach to and grasp each of the objects between the thumb and the four fingers of the right hand and then to lift and hold it. They were given no other instructions concerning how the objects were to be grasped, and subjects did not always grasp the objects in the manner that we had intended. (For example,

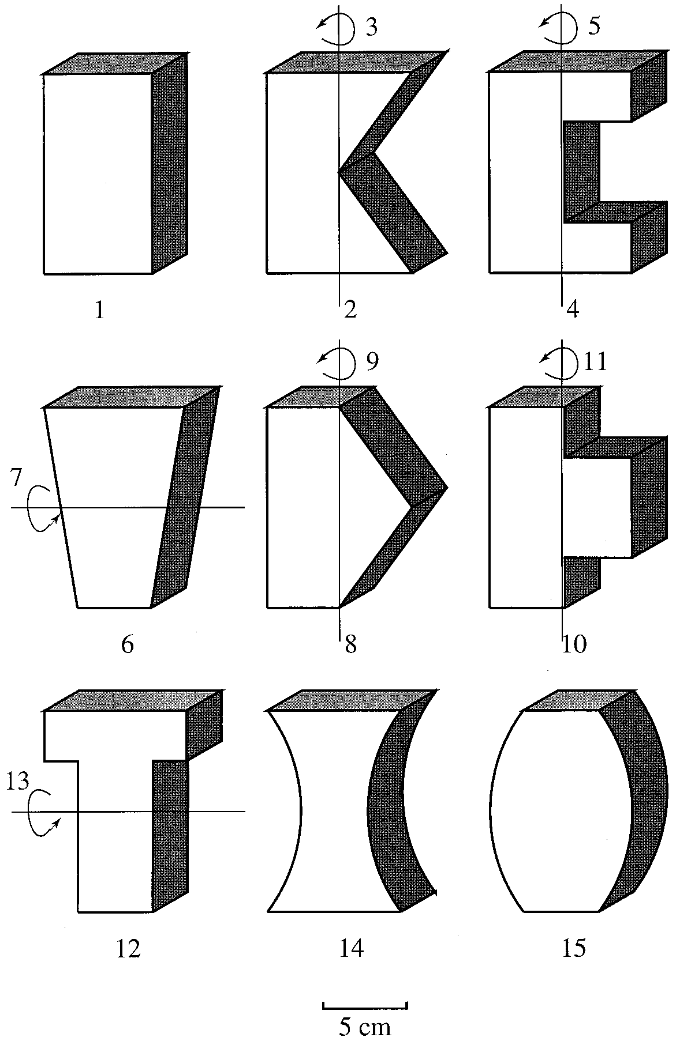

FIG. 1. Object shapes. Fifteen objects shapes used for the reaching and matching tasks are shown. Number at the *top* of some of the objects indicates the shape obtained by rotating the object along its vertical or horizontal axis.

some subjects grasped *objects 12* and *13* by placing all 4 fingers on the longer flat portion of the right face.) The hand and the object were in view throughout the trial.

Subjects began each trial with the elbow and wrist resting on a flat surface, the forearm horizontal, the arm oriented in the parasagittal plane passing through the shoulder and the hand in a semipronated position. They were asked to begin each trial with the hand in the same posture, e.g., thumb in contact with index and middle finger. The objects were ∼42 cm from the hand at movement onset. Each subject performed a total of 10 trials for each object shape, of which the last 8 were used for statistical analysis.

Before this set of trials, we asked subjects to shape their right hand into the posture appropriate for grasping the object while keeping the arm in a static position (Santello and Soechting 1997). A screen blocked the view of the right hand throughout this experiment. Data collection commenced after the subjects gave a verbal (‘‘ready’’) signal. We also obtained 10 trials for each of the shapes in this experimental condition and used the last 8 for statistical analysis.

Six right-handed subjects (3 males and 3 females) took part in the experiments, their age ranging from 29 to 43. All subjects gave informed consent and the protocols were approved by the Institutional Review Board of the University of Minnesota.

Experimental procedures and analysis

Hand posture was measured by resistive sensors embedded in a glove (CyberGlove, Virtual Technologies, Palo Alto, CA) worn on the right hand (Soechting and Flanders 1997). The degrees of freedom (df) measured at a resolution of <0.1° were the joint angles at the metacarpal-phalangeal (mcp) and proximal interphalangeal (pip) joints of the index, middle, ring, and little fingers (I, M, R, and L, respectively). Flexion was defined to be positive; the mcp and pip joint angles were defined as 0° when the finger was straight and in the plane of the palm. The motion of the thumb and wrist and the abduction angles of each of the fingers also were measured but not analyzed.

The output of the transducers was sampled at 12-ms intervals. For the matching task, 20 samples were averaged to define the static hand posture. For the reaching task, two switches were used to determine the onset and termination of the movement. The subject’s wrist contacted the first switch, and its release indicated movement onset, whereas the second switch was triggered when the object was lifted from the table, denoting the end of the trial.

Data from each trial were normalized in time (see Figs. 2 and 3) to facilitate a comparison of hand postures at different epochs during the movement. The main question to be addressed experimentally was the following: does the posture of the four fingers during the reaching movement reflect their posture at the time of contact, i.e., the shape of the object?

As already mentioned above, one would expect the middle and ring fingers to be more flexed (in comparison with the other 2 fingers) for concave objects. However, an overall flexion of the finger could be achieved by varying amounts of flexion at the mcp, pip as well as distal interphalangeal joints (Cole and Abbs 1986). We used discriminant analysis (Johnson and Wichern 1992) as a means to determine which of the degrees of freedom contributed most to define the posture of the hand as a function of object shape. Discriminant functions maximize the ratio of the between groups variance (**B**) to the within groups variance (**W**), in our instance the groups being the finger joint angles associated with each of the 15 object shapes. The discriminant functions $\mathbf{y}_i$ are computed from the eigenvectors $\mathbf{l}_i$ of the ratio $\mathbf{W}^{-1}\mathbf{B}_o$ of the between groups covariance matrix ($\mathbf{B}_o$) to the within groups covariance matrix (**W**)

$$\mathbf{y}_i = \mathbf{l}_i\mathbf{x} \tag{1}$$

where **x** is the eight-dimensional vector of hand posture (mcp and pip joint angles). The relative size of each eigenvalue (λ_i) indicates the relative importance of each of the discriminant functions; they were rank-ordered according to the size of λ_i. Hand posture on the kth trial then can be allocated to a particular object shape by first transforming the posture into discriminant space

$$\mathbf{y}_k = \mathbf{l}\mathbf{x}_k \tag{2}$$

and then determining the minimum distance d_{kj} between $\mathbf{y}_k$ and the group means $\mathbf{u}_j$

$$d_{kj}^2 = (\mathbf{y}_k - \mathbf{u}_j)^2 \tag{3}$$

Discriminant analysis was performed on the hand postures at different time periods of the reaching movement as well as on the hand postures used to match object shape.

The results of this analysis were used to construct a confusion matrix (Johnson and Phillips 1981; Sakitt 1980) that provides a summary of the extent to which hand posture at different epochs of the movement could predict the object that was grasped. Information theory (Shannon 1948) was used to quantify the extent to which the hand postures differed for different objects. The information transmitted by hand posture (h_p) about object shape (s) is given by

$$T(h_p, s) = H(s) + H(h_p) - H(h_p, s) \tag{4}$$

where

$$H(s) = -\Sigma p_i \log_2 p_i \quad (5)$$

and

$$H(h_p, s) = -\Sigma p_{ij} \log_2 p_{ij} \quad (6)$$

where p_i is the probability of the ith shape and p_{ij} is the joint probability of the ith shape and the jth hand posture. An absolute measure of performance is represented by the sensorimotor efficiency (SME) defined as the ratio between $T(h_p, s)$ (the information transmitted) and $H(h_p)$ (the maximum possible amount of information that could be transmitted).

To determine which hand shapes were most similar to each other, we rank-ordered the objects in the confusion matrix so that neighboring objects would be most likely to be confused with each other (see Fig. 8). This procedure involved minimizing the distance of off-diagonal entries in the matrix (weighted by their probability of occurrence) to the diagonal. In many instances, the off-diagonal elements were sparse, leaving uncertainty in the rank-ordering. Furthermore, the classification scheme described above does not take into account the confidence with which a particular hand posture can be assigned to a particular object shape. To overcome these deficiencies, we used a fuzzy-means clustering approach (Bezdek 1981). For the jth trial, with a hand posture $\mathbf{y}_j$ in discriminant space, we assigned weights w_{ij} for each of the i shapes to minimize

$$J = \Sigma w_{ij}^2 d_{ij}^2 \quad (7)$$

where d_{ij} is the distance to the ith shape (i.e., the group mean for that shape). The solution to this criterion is given by

$$w_{ij} = 1/\Sigma_k (d_{ij}/d_{ik})^2 \quad (8)$$

(A hard clustering is equivalent to minimizing $J = \Sigma w_{ij}\ d_{ij}^2$.) The fuzzy confusion matrices so created also were reordered to minimize the weighted distance of the off-diagonal elements to the diagonal.

We also used a cluster analysis to determine the extent of similarity or dissimilarity of the hand postures corresponding to the various shapes (Soechting and Flanders 1997). For this purpose, we used the data from the discriminant analysis.

RESULTS

Evolution of hand shape during the transport phase

Figures 2 and 3 show typical results from one subject (*SR*, 8 trials) for the motion of each of the fingers during the transport phase of the movement to two objects (*object 4*, Fig. 2, and *object 8*, Fig. 3). Movement time for each trial, which was typically 600 ms, has been normalized to 100. The traces depict the motion at the metacarpal-phalangeal joint (mcp, *left column*) and proximal interphalangeal joint (pip, *right column*) of each of the four fingers. (The symbol, bracketed by error bars, shown at the end of the movement refers to the average value for the matching task, which will be discussed later.)

As illustrated in Figs. 2 and 3, shortly after movement onset there was extension of all the digits, reaching a maximum between 30 and 70% of the movement duration. This initial extension was followed by flexion of all of the digits, to varying degrees, as the hand approached the object and as the object was grasped. This general pattern was found in all subjects and for all object shapes. The results shown in Figs. 2 and 3 are consistent with the description of the variation in finger span during reaching movements (cf. Jeannerod 1984; Paulignan and Jeannerod 1996) for tasks in which an object was grasped between the thumb and index or middle fingers. The intertrial variability of the angles at contact with the object was generally low (approximately ±5–10°) and constant throughout the latter half of the movement. On average, the SD for the 8 df computed at movement epochs ranging from 50 to 90% of movement time (in 10% increments) was only slightly larger than that at the end of movement (average ratio for all subjects was 1.15, with a maximum of 1.22 at 50% of movement time).

The posture of the hand at the end of the movement clearly depends on the shape of the object; Fig. 4 shows the average and SD of each of the df for the trials depicted in Figs. 2 and 3. For the concave object (*object 4*), the middle and ring fingers are more flexed at the pip joint than are the other two fingers. For this shape, at the mcp joint there is less variation in the amount of flexion among the four fingers, the middle finger being slightly more flexed than the other three. Conversely, for the concave shape (*object 8*), there is little variation in the amount of flexion at the pip joint for the four fingers, but the middle and ring fingers are more extended than are the other two fingers at the mcp joint. Thus the results for these two shapes conformed to the experimental design: concave shapes required more flexion at the index and little fingers and convex shapes more flexion at the other two fingers. However, as Fig. 4 illustrates, for some objects the conformation of the fingers at the mcp joint was more clearly related to the object's shape; for other objects, it was the conformation of the fingers at the pip joint.

The results illustrated in Figs. 2–4 were generally representative of the results from this subject for the other concave (*objects 2* and *14*) and convex (*objects 10* and *15*) shapes. There was a high degree of similarity for the pattern of flexion at the various joints for shapes 2 and 4 (the 2 concave shapes with corners) as well as for the two convex shapes with corners (*8* and *10*). For the two shapes with curved surfaces (*14* and *15*) there appeared to be a pattern of modulation at both the pip and mcp joints. Qualitatively, each of the six subjects had different patterns of hand postures for different shapes, but the patterns were idiosyncratic to each subject. For example, one other subject showed a pattern similar to that illustrated in Figs. 2–4. In another subject, there was a pattern of modulation at both the mcp and the pip joints for convex and for concave shapes. In another subject, there was a general tendency, irrespective of the object to be grasped, for increasing amounts of extension at the pip joints from the index finger (most flexed) to the little finger (most extended).

Thus in accordance with experimental design, differently shaped objects were grasped with hand postures that were distinct. We come now to the main question we wish to address in this paper: are the hand postures distinct also well before contact is made with the object? From the examples shown in Figs. 2 and 3, the answer to this question is not clear because the extent of the motion at each of the df after the time of maximum hand aperture was variable from joint to joint and from object to object. For example, for the concave object (Fig. 2), the amount of flexion after maximum aperture (>60% of movement time) was largest for the middle finger and the ring finger, particularly at the pip joint. In fact the pip joint of the index finger moved almost imperceptibly. Conversely, for the convex shape (Fig. 3), after the time of maximum aperture, the greatest amount of motion occurred at the pip joint of the little finger. In contrast

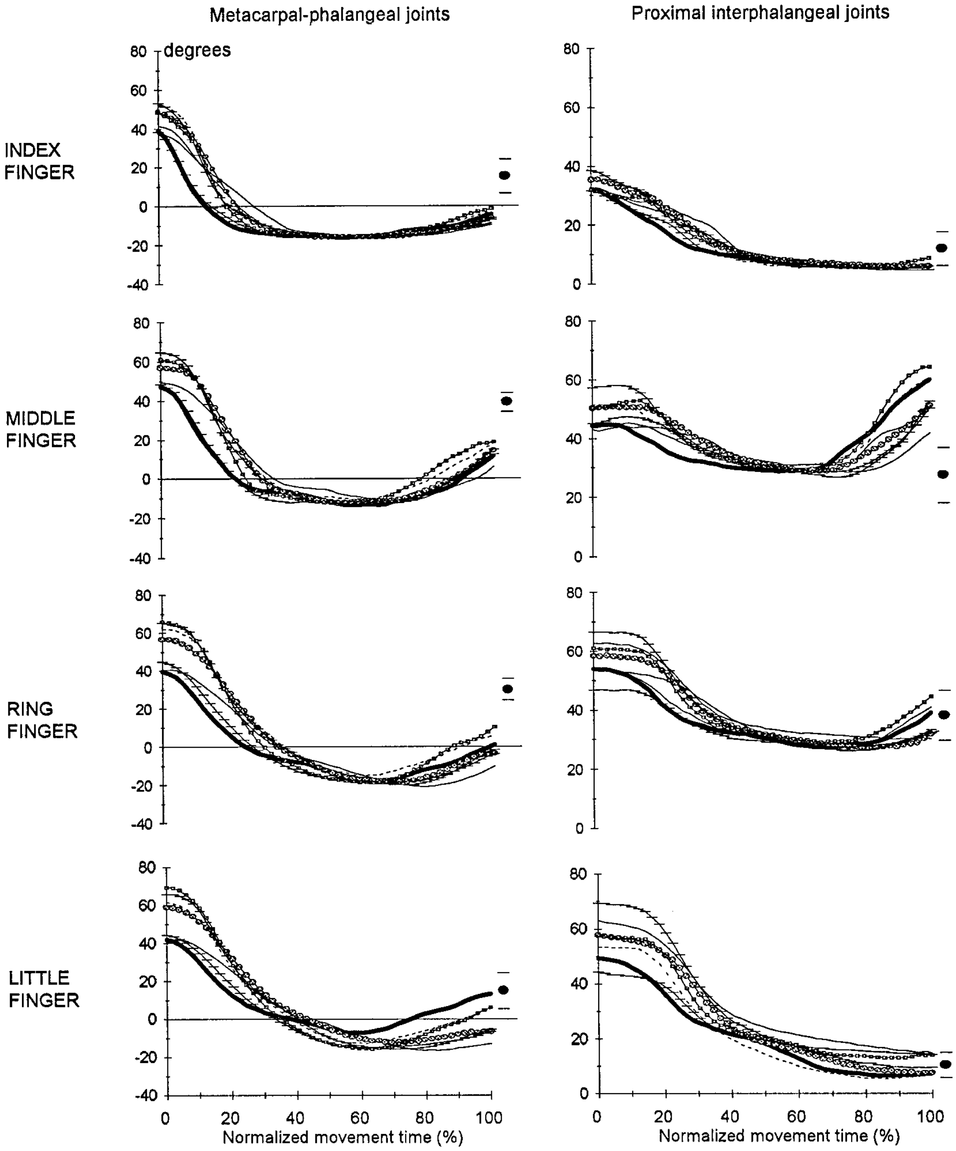

FIG. 2. Time course of motion at the metacarpal-phalangeal (mcp) and proximal interphalangeal (pip) joints during a reaching and grasping movement. Each of the traces depicts the motion at the mcp joints (*left*) and at the pip joints (*right*) of the fingers for one trial. Data for all 8 trials that entered into subsequent analysis are presented. Positive and negative values denote flexion and extension, respectively. Data are for 1 subject (*SR*). Object grasped was concave (*object 4*). Duration of each reaching movement was normalized (0 and 100 on the *x* axis represent the onset and termination of the reaching movement, respectively). Symbol shown at the end of the reaching movement is the average value for the matching task ± SD.

to the pattern in Fig. 2, in Fig. 3 the amount of flexion at each of the mcp joints (after $t = 50\%$) was small and appeared to be about the same for each of the fingers.

Qualitatively it thus appears that there may be some correlation between the posture of the hand during the movement and the posture of the hand at movement's end, but that this correlation is not overly strong and not the same for all df. This was borne out by a regression analysis on the relation between the minimum angle (generally, the angle at maximum hand aperture) of each df for all object shapes and the angle at contact with the object. Figure 5 shows the correlation coefficients (r) of each df averaged across subjects (■). For each of the df, the correlation coefficients are positive, with higher r values for the mcp angles (0.75–0.90) than for the pip angles (r values ranging from 0.37 to 0.66). This quantitative analysis is consistent with the results shown in Figs. 2 and 3: there was more variability in the amount of flexion at the pip joints than at the mcp joints as the hand approached the targets.

The degree of correlation between the minimum angle of each df and its value at contact with the object does suggest that the hand shapes for different objects differed at the time of maximum hand aperture. This conclusion is supported by the results presented in Fig. 6, which shows the variation in each of the joint angles for one subject (*MS*) at four different stages of the movement (50, 70, 90, and 100% of movement duration). At each epoch, the angles at the mcp joints (Fig. 6, *left*) and the pip joints (Fig. 6, *right*) are plotted as a function of the objects to be grasped (x axis). The shapes were ordered according to the criterion also used to order the objects in Fig. 10. In this ordering, there is a progression from convex to concave shapes, with the flat vertical shapes in between. To facilitate a comparison among different time periods, we computed the minimum angle for each df for the 15 shapes at each point in time and used this value as the baseline (0°).

As noted above, the hand postures at contact (Fig. 6, *top*) were clearly distinguishable among each other. This was particularly clear at the mcp joints: for the left-most shape, the angles for the four fingers have a concave upward distribution, with the flexion at the index and little fingers being greater than the flexion at the other two fingers. For the

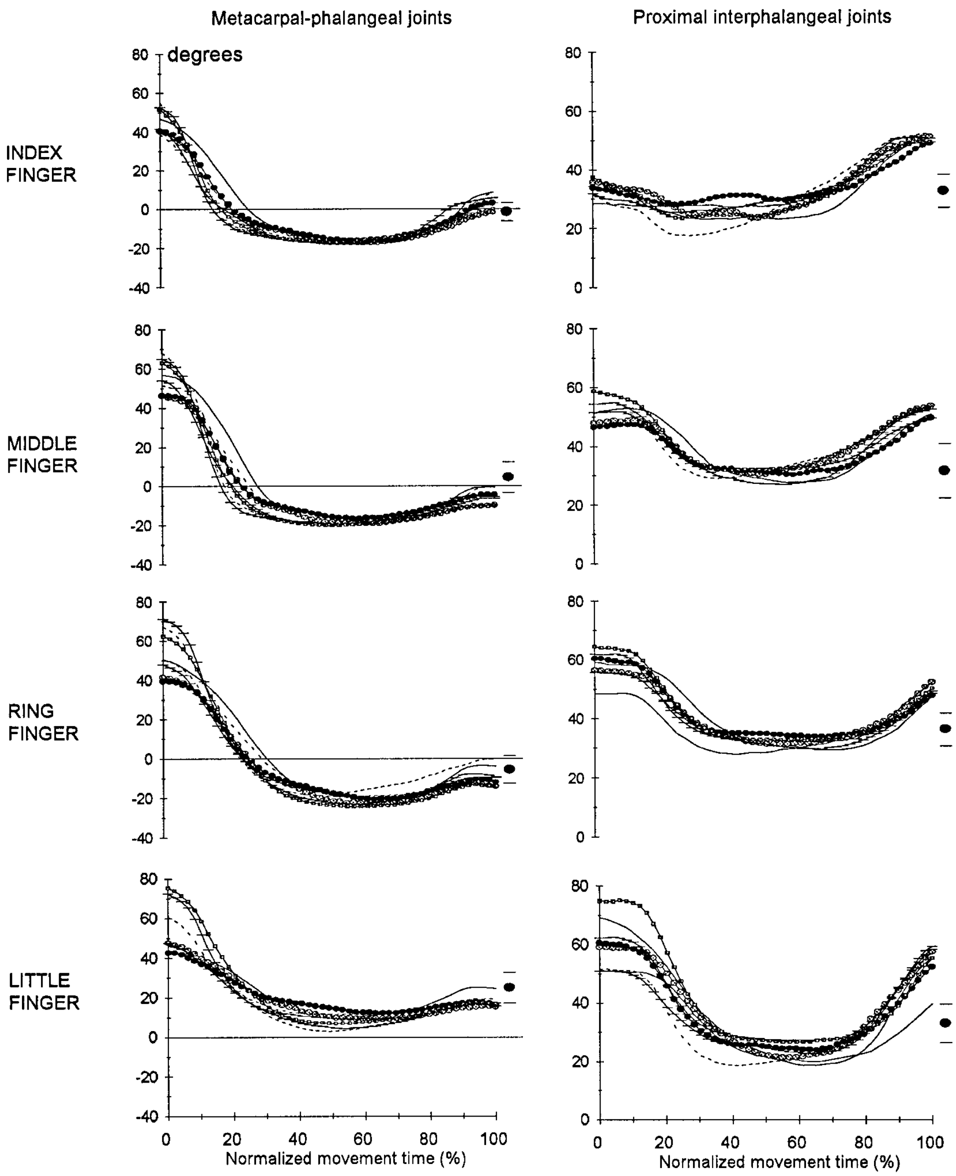

FIG. 3. Reaching and grasping a convex object. Traces depict the motion of the fingers for movements in which a convex object (*8*) grasped. Data are from the same subject (*SR*) as those in Fig. 2.

right-most shape, the trend is in the opposite direction: the four angles have a convex downward distribution, with the flexion at the middle and ring fingers being larger. Shapes arrayed in between these two extremes show a gradual metamorphosis from one distribution to the other. At 90% of movement time, the patterns are largely similar to those at contact, and, while the patterns at 50% of movement time (Fig. 6, *bottom*) are not as distinct, one can nevertheless observe similarities between the patterns at 50% of movement time and at contact.

The extent to which the hand shape at different epochs is correlated with the hand shape at contact is summarized in Table 1. For the purposes of this analysis, the amplitude of each hand posture was normalized by first assigning the value of zero to the mean amplitude of all the 8 joint angles and then expressing the amplitude of each df as a standard deviation of the mean amplitude. An r value was computed for each object, and these then were averaged. The r values increase as the hand approaches the object, but it is clear from the size of their standard deviations that the extent to which hand shape at different epochs is correlated depends on the object to be grasped.

Discriminant analysis of hand shape

The impressions gleaned from Fig. 6 and the positive correlation between hand posture during the movement with the hand posture at contact (Fig. 5 and Table 1) suggest that, after peak hand aperture is reached, distinct hand shapes corresponding to different objects emerge gradually. Because the objects were chosen to differ primarily in shape (i.e., convexity vs. concavity), one is tempted to conclude that hand shape after the time of peak aperture reflects the shape of the object to be grasped. The conclusion is a bit premature because there may be differences in the apparent sizes of the objects. It is well known that hand aperture varies with object size, and it is also possible that hand shape varies with object size. The analysis in this section was meant to rule out this possibility.

As was shown in Figs. 2 and 3, the amount of flexion at

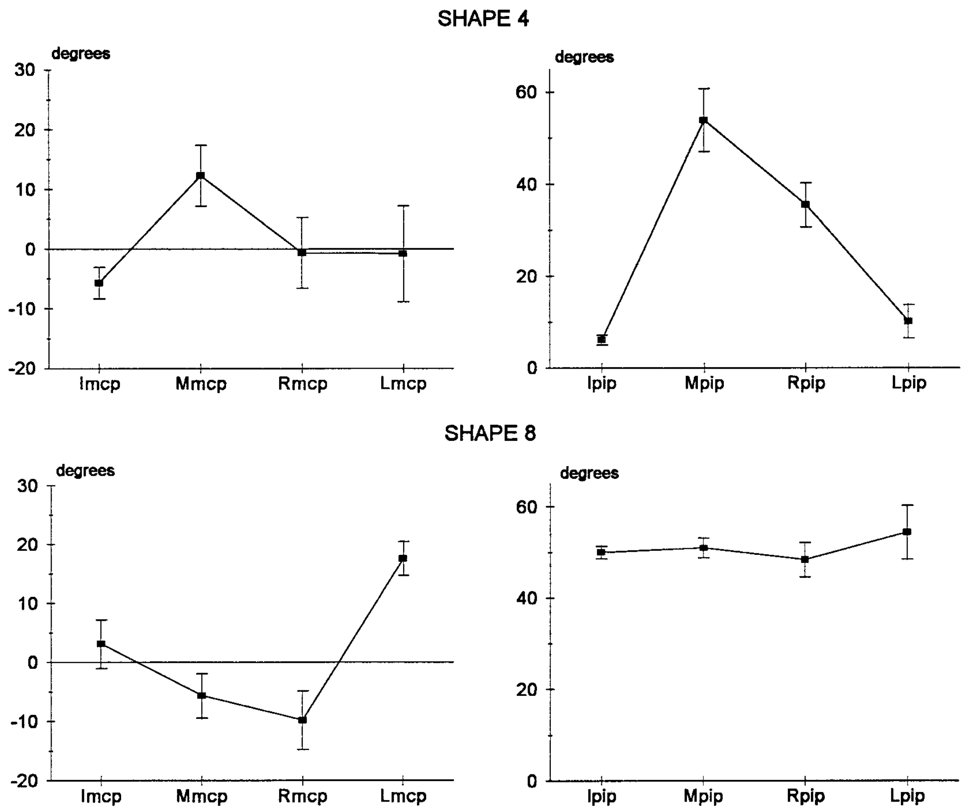

FIG. 4. Hand posture at contact with concave (*top*) and convex (*bottom*) objects. Angles at mcp (*left*) and pip (*right*) joints of each of the fingers are shown for the same subject (*SR*) as in Figs. 2 and 3 for 2 objects. Data shown are averages of 8 trials ± SD. Note that the pip joints of the middle (M) and ring (R) fingers are more flexed for the concave object (*top*) and that the mcp joints at the index (I) and little (L) fingers are more flexed for the convex object.

the mcp and the pip joints at the several fingers could differ for different shapes. Also, different subjects could show different patterns. Thus, a priori, it is not clear which of the df of the fingers, or which combination, is most effective in differentiating among different hand shapes. Discriminant analysis provides the solution to this dilemma. As described in METHODS, discriminant analysis provides a set of ordered functions that accentuate the distinction in hand shapes for the several objects. The discriminant functions can be arranged in order of importance. In our case, where there were 8 df, there were eight discriminant functions, each a linear combination of the df. For each subject, a set of discriminant functions was computed from the hand postures measured at different time epochs of the movement, i.e., at 50, 60, 70, 80, 90, and 100% of the movement time. For all subjects, the first three functions could explain >85% of the variance (VAC), with no significant trend in VAC with movement time.

The weighting coefficients of the first two functions from two subjects are shown in Fig. 7. The first discriminant

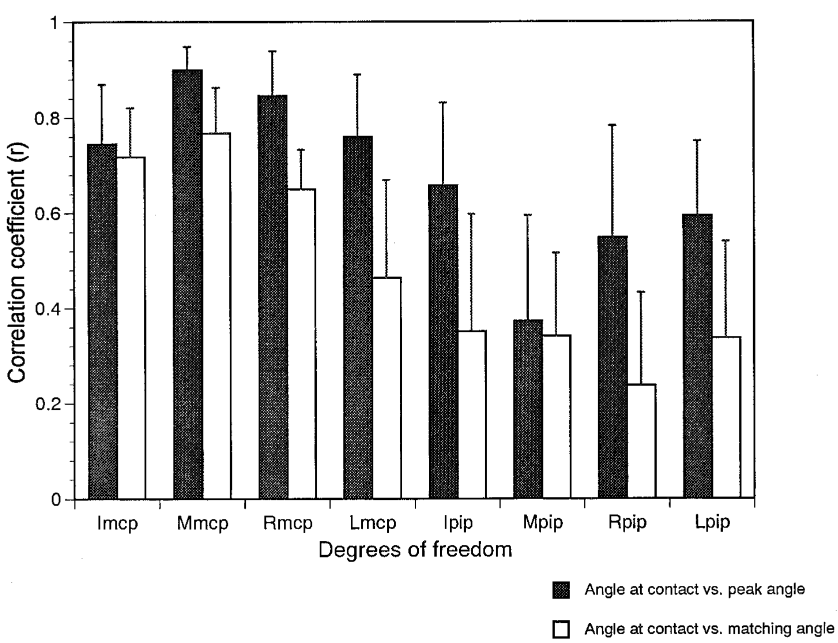

FIG. 5. Correlation between angle at contact vs. peak angle and matching angle for each of the degrees of freedom. Correlation coefficients (r) between the angle at contact and the peak angle (■) and the angle in the matching task (□) are shown. r values shown were averaged across subjects (vertical bars are SD). An r value > 0.641 is significant at $P < 0.01$.

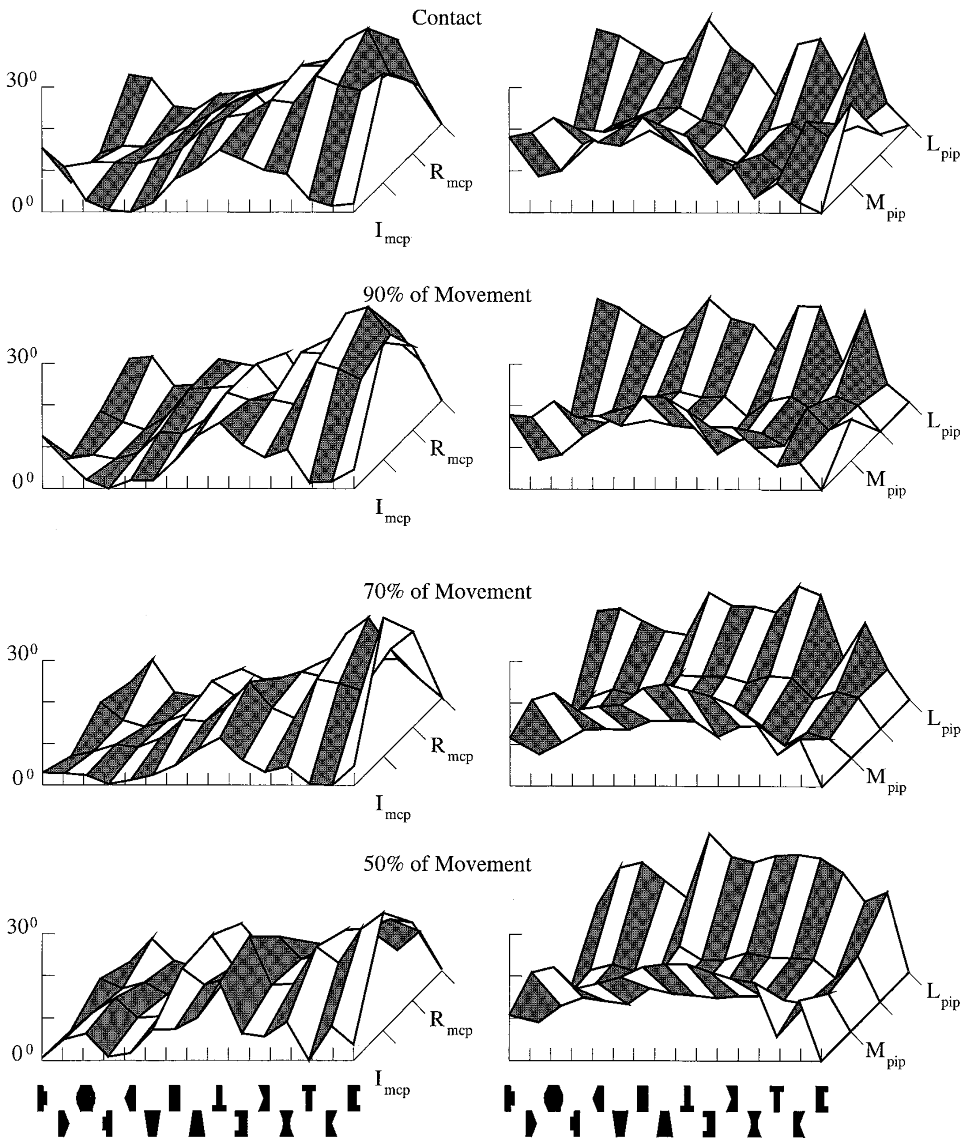

FIG. 6. Evolution of hand shape during reaching. Hand postures measured at different epochs during the movement (50, 70, 90, and 100% of movement time) are illustrated for each of the objects. Data are from a different subject (*MS*). Objects are arranged on the horizontal axis, with a progression from convex shapes (*left*) to concave ones (*right*). Oblique axis denotes the 4 df at the mcp joints (*left*) and the pip joints (*right*). Value 0° denotes the minimum value (most extended posture) for the 15 objects at each df.

function for both subjects (accounting for 74% of the variance for *FC* and 52% of the variance for *MF*) is highly consistent across epochs. For *subject MF,* the second discriminant function also shows a fairly high degree of consistency, whereas the one for *FC* is smaller and more variable. It is also clear that the shape of the first discriminant function is quite different between the two subjects (Fig. 7, *top left* and *right*). The shape of the first discriminant function for *subject FC* can be related readily to the convexity/concavity scale of the objects to be grasped: the mcp and pip angles of the middle two digits are weighted positively, whereas the angles at the index and little fingers are weighted negatively. [Because convex shapes should require more flexion at the outer two fingers and concave shapes should require more

TABLE 1. *Correlation coefficients of the relationship between hand postures during reaching and hand posture at contact*

Subjects	Normalized Reaching Duration (%)				
	50	60	70	80	90
FC	0.923 ± 0.042	0.932 ± 0.040	0.953 ± 0.029	0.980 ± 0.014	0.994 ± 0.005
GB	0.798 ± 0.138	0.832 ± 0.136	0.873 ± 0.120	0.913 ± 0.092	0.966 ± 0.038
MF	0.665 ± 0.237	0.676 ± 0.237	0.705 ± 0.227	0.760 ± 0.200	0.883 ± 0.122
MS	0.620 ± 0.198	0.741 ± 0.184	0.826 ± 0.150	0.876 ± 0.117	0.948 ± 0.056
SR	0.834 ± 0.172	0.858 ± 0.163	0.873 ± 0.144	0.912 ± 0.113	0.971 ± 0.045
UH	0.981 ± 0.014	0.976 ± 0.012	0.977 ± 0.013	0.982 ± 0.010	0.994 ± 0.003

The correlation coefficients (r) of the relationship between the hand postures (8 df of the fingers) at different epochs of the movement and the hand posture at contact were calculated for each subject and each object. The amplitude of the hand postures was normalized before performing the regression analysis. The rs shown are the averages of 15 values for each subject ±SD. An r value >0.834 is significant at $P < 0.01$.

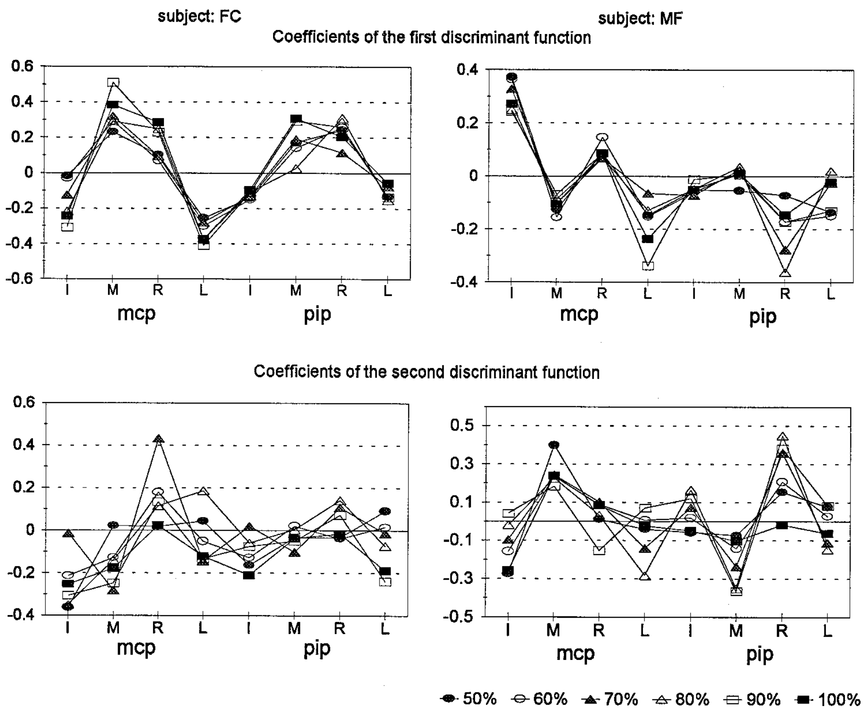

FIG. 7. Coefficients of the discriminant functions at different epochs for 2 subjects. Coefficients of the 1st 2 discriminant functions for each of the df of the fingers are shown for 2 subjects: *FC* (*left*) and *MF* (*right*). Each symbol refers to a given epoch of the reaching movement, as indicated by the label. Note the degree of reproducibility of the 1st discriminant function at all epochs of the movement.

flexion at the middle two fingers, the weighted difference between the angles of the outer two fingers (I and L) and the angles of the inner two fingers (M and R) could function as an index of convexity.] The first discriminant function of two others subjects (*SR* and *MS*) resembled the one shown for *subject FC.* The pattern for *subject MF* was more difficult to intuit, as was the pattern for the final two subjects.

The discriminant functions were used to classify hand postures. In discriminant space, we computed the mean of the eight trials for each object and then we classified individual trials as corresponding to the closest object mean. Figure 8 shows the ''confusion matrices'' of the hand postures (measured at 50, 70, and 100% of the movement duration) that result from this analysis for *subject MS.* The number of trials that was predicted to correspond to each object is listed along the columns, and the row denotes the object that was the actual target for that trial. If hand shape were a perfect predictor of the object to be grasped, all of the entries would lie on the diagonal. The frequency of each off-diagonal entry provides an indication of the extent to which the hand posture was similar for the two shapes.

The matrix in Fig. 8, *top left,* shows the results for hand postures taken at the midpoint of the movement. The order in which the shapes are arrayed in this matrix is arbitrary. In Fig. 8, *top right,* we have rearranged the same data, now grouping shapes that were most likely to be confused with each other closer together. This was done by minimizing the distance of all off-diagonal entries (weighted by their frequency of occurrence) from the diagonal. Thus at 50% of movement time, the postures for *objects 15, 7, 1,* and *5* (the *first 4 columns* of the matrix) were highly similar to each other, as were *objects 2* and *4* (the *last 2 columns*) and *objects 3, 6,* and *14.* The matrices in the lower row of Fig. 8 show that the amount of confusion decreased with time, i.e., hand shape at 70% of movement time and at the time of contact with the object was more likely to correctly predict the object that was grasped.

The extent to which hand shape correctly predicts the object to be grasped can be quantified by using information theory; the information transmitted by hand shape indicates the number of objects that are actually discriminated, on a logarithmic scale. In Fig. 9, we present the SME, the amount of information transmitted normalized by the maximum amount possible ($3.91 = \log_2 15$). For this subject (*MF*), SME increased monotonically as time progressed, reaching a maximum value of 86% (10.3 objects) at contact. The results shown in Fig. 9 were typical (Table 2). In all but one subject (*UH*), SME increased monotonically as time progressed. (For this exceptional subject, where SME decreased at 70 and 80% of movement time, there was a 25% increase in the SDs of the finger angles compared with other times.) On average, at 50% of the movement duration the SME was 70%, indicating that hand posture at the movement's midpoint already transmitted ~2.74 bits of information (equivalent to 6.7 different objects).

Ordering and clustering of object/hand shape

We now will demonstrate that the different hand postures at a given epoch of the movement actually reflect the *shape* of the object to be grasped, i.e., its convexity or concavity. We will do this by showing that hand postures for convex objects are similar to each other and dissimilar to those for concave objects. One indication of the extent to which hand postures are similar to each other is given by the ordering of objects in the confusion matrices shown in Fig. 8. Because many of the entries in these matrices are sparse, the ordering is not entirely reliable. For example, at contact, all of the off-diagonal entries for *objects 4* and *10* are zero. These objects are arrayed next to each other in the matrix, but this arrangement is arbitrary. Furthermore, the hard clustering in Fig. 8 overstates the reliability with which hand postures can be classified because the probability of belonging to a class is either 0 or 1 (if it is closest to that class). A method

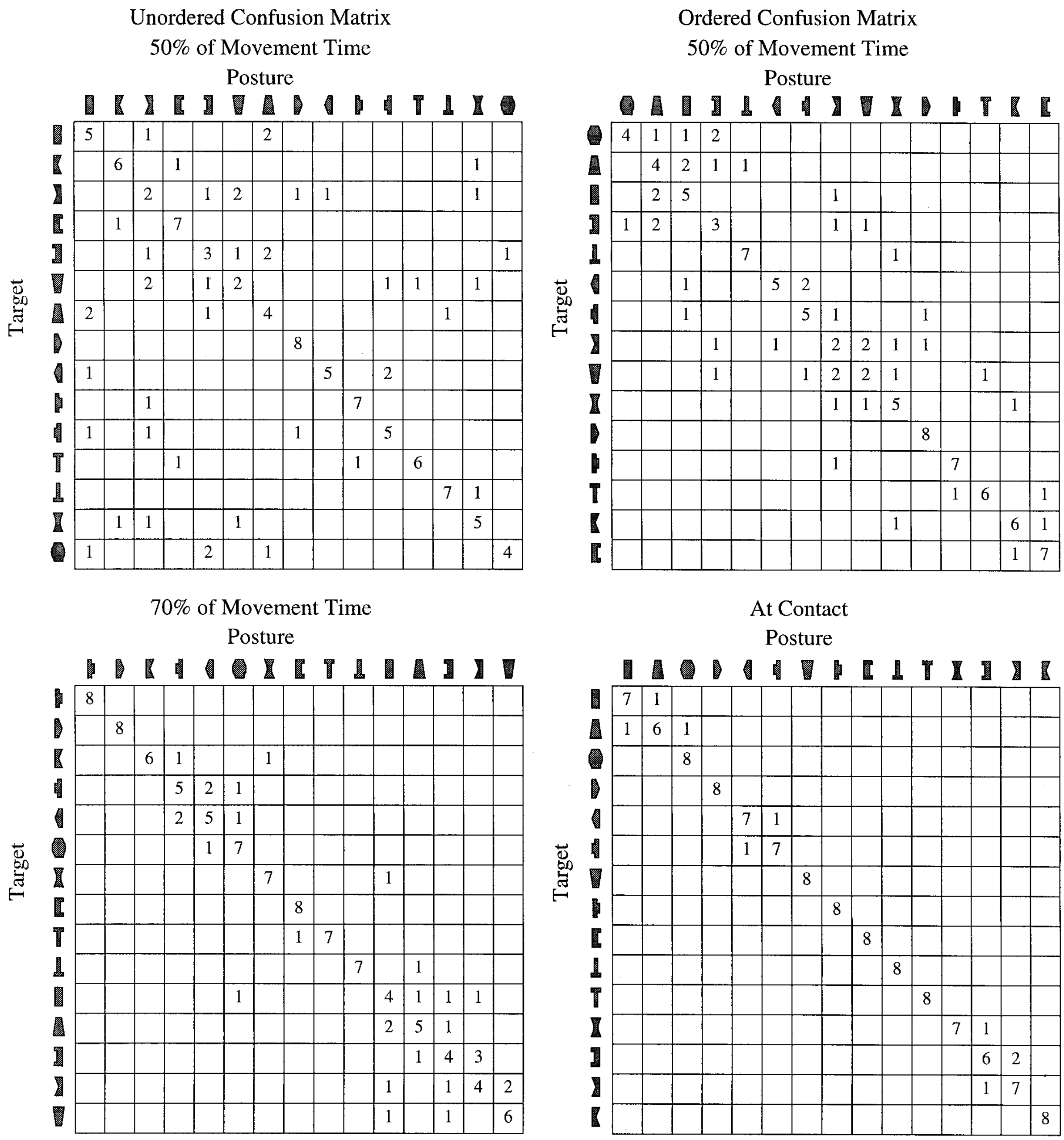

FIG. 8. Classification of hand postures using discriminant analysis. ''Confusion matrices'' at different epochs of the movement indicate the extent to which hand posture can predict the object to be grasped. Numbers in each cell denote the numbers of trials for movements to a particular target (row) that are allocated to a given object (column). Ordering of the matrix at *top left* is arbitrary. Objects in the other 3 matrices have been ordered so as to bring nonzero off-diagonal entries as close as possible to the diagonal.

that overcomes these objections is to use a fuzzy clustering criterion, according to which the probability of belonging to a particular class is related inversely to the distance from that class, but is never 0 (see METHODS). The results of this analysis, for the same data as in Fig. 8, are shown in Fig. 10. The shading in each square indicates the probability according to which a given posture corresponds to a particular target object. The objects are again ordered using the same criterion as in Fig. 8. From this figure, it is again clear that the discrimination among hand postures increases with time.

From the ordering in Fig. 10, it is clear that hand posture at contact is related to the convexity or concavity of the object. All of the concave shapes (*4, 2, 12,* and *14*) are arrayed at the *right* of the matrix, all of the convex shapes (*10, 8,* and *15*) are arrayed at the *left*, and the flat shapes are in between. The ordering is virtually the same at 90% of the movement time and is still largely preserved at 70% of movement time (where anomalously, the convex *object 10* is arrayed among the concave ones on the right). For this subject, the ordering of the objects according to shape is indistinct at 50% of movement time.

In general, the ordering of the shapes was highly correlated across movement times for all subjects. We assigned

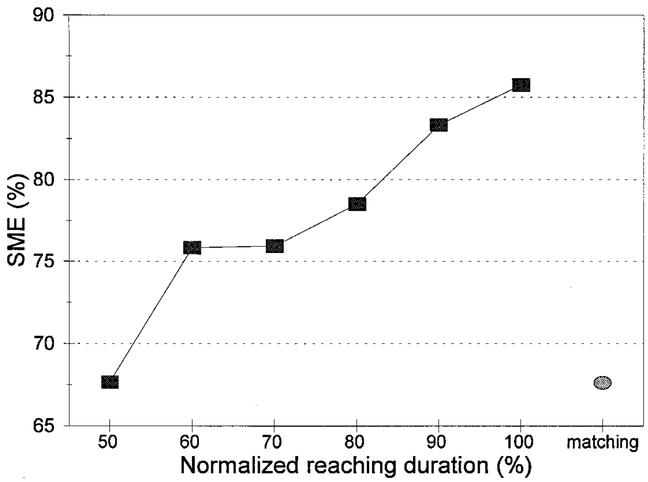

FIG. 9. Sensorimotor efficiency (SME) at different epochs of the reaching movement. SME indicates the amount of information transmitted by handshape about the object to be grasped, normalized to the maximum amount of information that could be transmitted. Data are for 1 subject (*MF*). ⊗, SME during the matching task.

a rank order to each shape according to its order of appearance in the matrix and computed a correlation coefficient between the ordering at various times. For the results in Fig. 10, this analysis gave *r* values that were significant ($P < 0.05$) when the ordering at 70, 80, and 90% was compared with the ordering at movement's end. For the other two times (50 and 60%), the correlation was positive but not significant. For the other five subjects, the correlation between the ordering of objects shapes at 50% of movement duration and at contact was positive and significant. At all times thereafter as well, this analysis gave positive *r* values, with those for at least four of the six subjects reaching significance.

An alternate way to assess the extent to which hand shape is related to the shape of the objects on a convexity/concavity scale is shown in Figs. 11 and 12. In Fig. 11 the same data as in Figs. 8 and 10 are now plotted in the space of the first three discriminant functions. [Although the classification of hand postures shown in Fig. 8 was based on the whole set of discriminant functions ($n = 8$), the first 3 functions were found to explain ~85% of the variance. Therefore, they are sufficient to capture the main features of the data.] Each point in the plots denotes the average value of the hand posture for the indicated object.

Considering first the data at movement's end (Fig. 11, *bottom*), one finds that the points corresponding to the convex shapes are arrayed to the *right* on the first discriminant axis, whereas the concave shapes fall on the *left* on this axis. The flat shapes fall in the *middle,* and much of the discrimination among them appears to be provided by the second and third discriminant functions. The first discriminant function provides a clear convexity/concavity gradient at other movement times as well. At 90, 70, and 50% of movement time, the concave *object 4* falls in the *top right corner* of each plot, and the convex *objects 8* and *10* are located close to the *left edge* of each of the panels. (The weighting coefficients for the first discriminant function, which strongly resembled that for *FC* in Fig. 7, reversed between 90% of movement and contact. Accordingly, the order of progression from convex to concave also reverses.)

Figure 11 shows that the hand postures for some objects are already quite distinct at 50% of movement time because they are well segregated from the other points. For other objects, the points are clustered close together. As time progresses, the separation for the points corresponding to the various targets increases, in accord with the finding (Fig. 9) that the amount of information transmitted by hand posture about the object increases with time.

The cluster diagrams in Fig. 12 provide a visualization of the distances separating pairs of points in discriminant space. The vertical axis indicates the distance separating two branches on the tree, distance having been computed from the full set of eight discriminant functions and having been normalized according to the maximum distance between all pairs of points. Where the branches join, the location of the two branches is replaced by their geometric mean. The diagrams reinforce the conclusion presented earlier: already at 50% of movement duration, most of the concave (*objects 2, 4, 12,* and *13*) and convex (*object 10*) are well segregated from the other shapes. Furthermore, the various shapes do not appear to fall into two or three distinct clusters.

Matching object shape

The amplitude of each df for the matching task is shown in Figs. 2 and 3 as symbols at the end of the reaching movement. In this subject, as well as for all the other subjects, we found that the flexions at the mcp and pip df were generally larger and smaller, respectively, in the matching task. In other words, subjects tended to assume a more flexed posture at the mcp joints, and one that was more extended at the pip joints than when actually grasping the objects.

We performed regression analysis on the df from actual (at contact) and virtual (in matching) hand postures to assess the extent to which the two postures differed. Figure 5 shows the *r* values averaged across all subjects (□). Greater *r* values were found for the mcp than for the pip df, the former ranging from 0.463 to 0.767. The coefficients of the discriminant functions also were found to be larger for the mcp df than for the pip df, indicating that subjects primarily modulated the angles at the mcp df when performing the matching task.

TABLE 2. *Sensorimotor efficiency during reaching and matching*

	Normalized Reaching Duration (%)						
Subjects	50	60	70	80	90	100	Matching
FC	78	83	88	84	96	89	67
GB	50	52	57	61	63	71	42
MF	68	76	76	79	83	86	68
MS	65	75	77	84	93	92	80
SR	75	78	82	86	86	90	80
UH	84	86	76	79	85	87	68

The sensorimotor efficiency (SME) at different epochs of the reaching movement and for the matching task was computed for each subject. The amplitude of the SME index increases during reaching, with a maximum value at contact with the object. The information transmitted for the matching task is lower than at contact with the object. This indicates that the discrimination among hand postures was higher when grasping the objects than in matching their shapes.

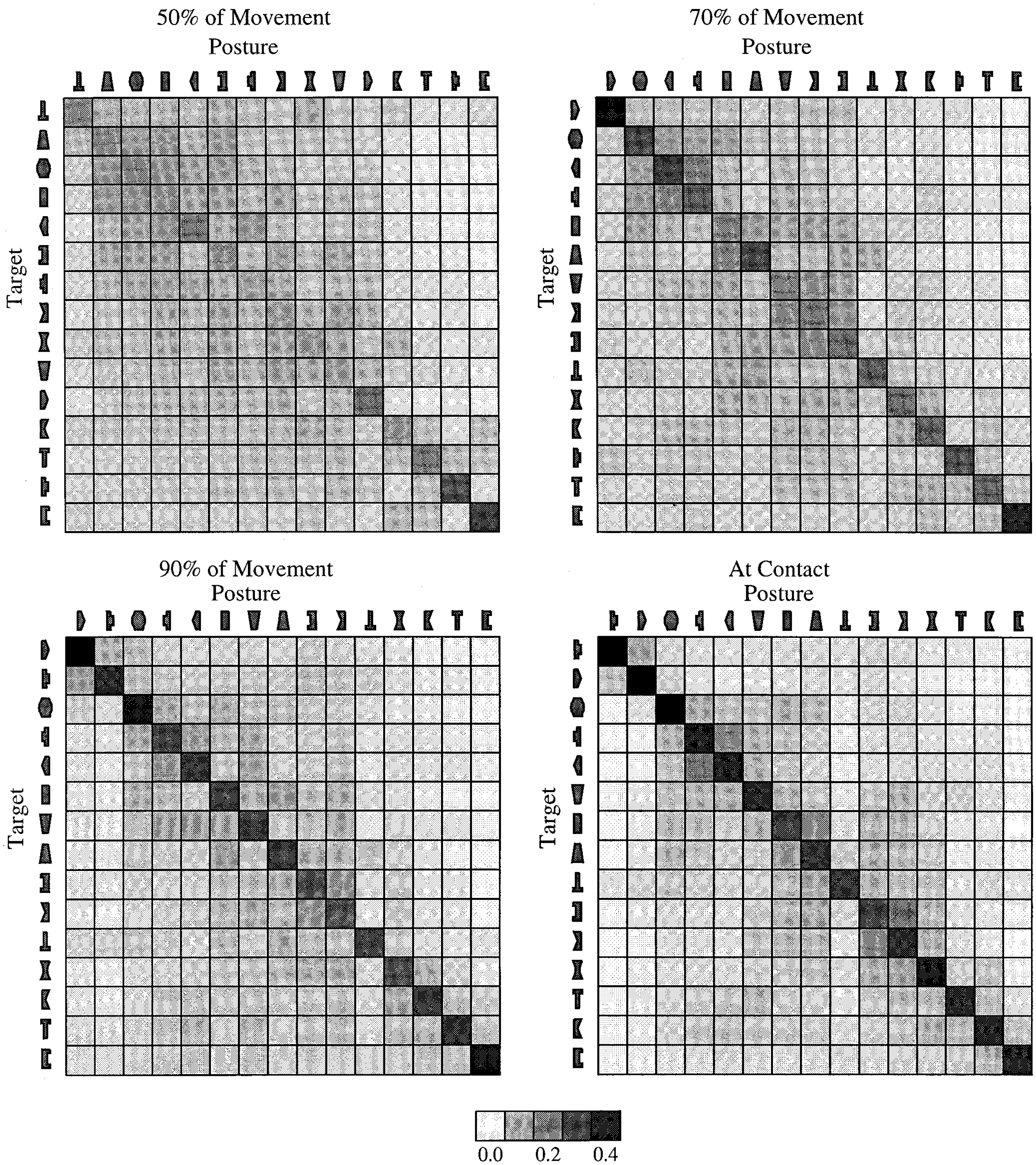

FIG. 10. Confusion matrices obtained by using a fuzzy clustering algorithm. Data shown are for the same subject as those in Fig. 8 now with a fuzzy clustering criterion. Probability with which a given hand posture was assigned to each object is coded by the darkness of each entry, the darkest shade indicating the highest probability (see scale at *bottom*).

The confusion matrices of the virtual postures were characterized by a greater scatter along the main diagonal. Table 2 shows the SME index of the matching hand postures, together with the SME index of the hand postures at the time of contact with the object for comparison. The SME for the matching task was lower than the SME for grasping in all subjects. One factor that could account for the decreased information transmitted about object shape during the matching task is increased trial-to-trial variability. Averaged over all subjects, 8 df and 15 objects, the SD was 2.4 times as large as that computed for the postures when subjects actually grasped the objects.

DISCUSSION

We have shown here that as the hand approaches an object that is to be grasped, its shape is gradually molded to conform to the shape of the target. We provided both qualitative as well as quantitative evidence in support of this conclusion. Qualitatively, Fig. 6 demonstrates that the pattern of flexion at the mcp and pip joints of the fingers evolves gradually and that some aspects of the pattern are already evident at the midpoint of the transport phase. We also showed that there was a positive correlation between the angles of each of the df at maximum aperture ($\sim$50% of movement dura-

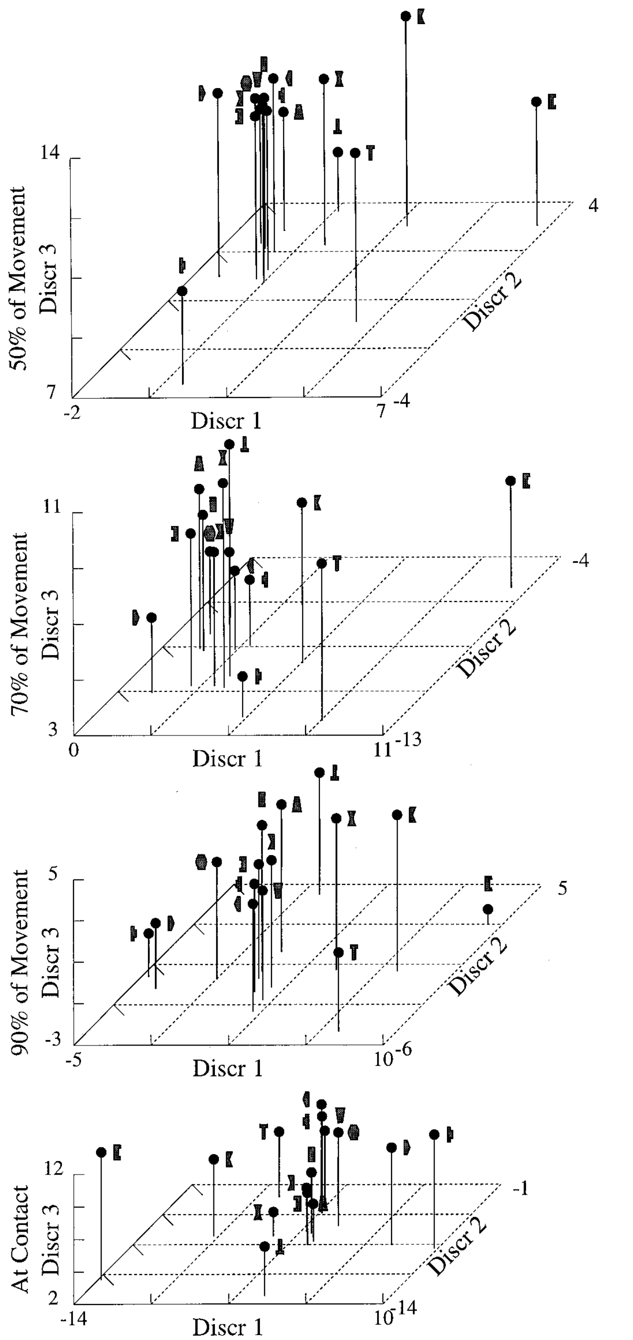

FIG. 11. Distribution of hand postures in discriminant space. Mean value of the hand postures for each of the 15 objects is plotted in discriminant space (1st 3 discriminant functions). Data are from the same subject (*MS*) as those in Figs. 8 and 10. Distance between the values of 2 points in discriminant space provides a measure of the extent to which pairs of hand postures were dissimilar to each other.

tion) and at the time the object is grasped (Fig. 5). Moreover, we showed a gradual increase in the information that is transmitted by the hand's conformation about the particular object that is to be grasped (Fig. 9 and Table 2).

Several lines of evidence point to the conclusion that it is the shape of the object (i.e., whether it presents a flat, concave, or convex surface to the fingers) that is being discriminated rather than some other characteristic of the objects (such as the size necessary for grip). We ordered the objects, grouping those with the most similar hand shapes close together (Fig. 10) and found that convex objects tended to be grouped with other convex objects and similarly for concave objects. This ordering already was present to a large degree at the midpoint of the transport phase (Figs. 10–12). The form of the discriminant functions (Fig. 7) also supports the conclusion that the hand postures during the movement reflect the shape of the object, albeit incompletely. The difference in the amount of flexion at the index and little finger (taken together) relative to the amount of flexion at the ring and middle fingers should distinguish between most convex and concave objects. Accordingly, one would expect a discriminant function that assigned positive weights to the middle and ring fingers and negative weights at the other two (either at the mcp joints or the pip joints or both) to be most effective at differentiating between convex and concave shapes. For at least some subjects (Fig. 7), this expectation was met. Furthermore, the form of the first discriminant function changed little with time, implying that hand shapes were discriminated according to similar criteria at the movements' midpoint as well as at the time of contact with the object.

The information transmitted by the posture of the hand about the object to be grasped increases gradually throughout the movement. Note that we began our analysis at the movement's midpoint, i.e., at a time when maximum hand aperture had generally been achieved. Thus the lesser amount of information transmitted about object shape (at 50–80% of

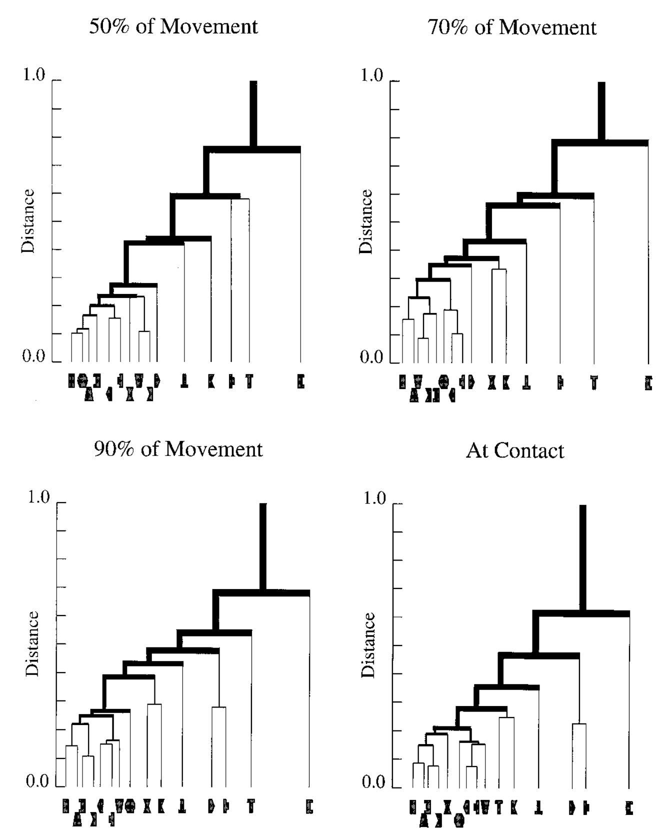

FIG. 12. Clustering of hand postures as a function of object shape. Cluster analysis was used as an alternative way to represent graphically the discrimination among hand postures. Vertical axis indicates the normalized distance between pairs of points in discriminant space (Fig. 11). Height of the branch points of the tree indicates the degree of similarity between the 2 branches.

movement duration) is not because the fingers are still extending from their common starting posture. Furthermore, increased variability of hand postures at intermediate stages of the movement also cannot account for the lesser amount of information transmitted at these intermediate stages of the transport phase. In fact, the standard deviation of the finger angles remained just about constant from 50% of movement duration to the time of contact.

Thus the conclusion seems inescapable that the hand is only gradually molded to the shape of the object to be grasped, as the movement progresses. Stated another way, one can surmise that the specification of hand shape is incomplete at the time of maximum hand aperture. The studies of Ghez and colleagues (Favilla et al. 1989, 1990; Ghez et al. 1997) also suggest that the specification of some movement parameters evolves gradually. They presented subjects with information about movement direction and amplitude and forced the subjects to initiate the movement at variable times after the information had been presented but before their normal reaction time. They found that the specification of amplitude and direction of the movement both evolve gradually but independently of each other.

Other studies suggest that some parameters are specified fully at the time of movement initiation, whereas others evolve more gradually. In recordings from premotor cortical areas in a task that involved the control of movement amplitude as well as direction, Fu et al. (1995) found that these neurons encoded information about several parameters, namely movement direction and distance and the location of the target. Before the movement's onset and early on in the movement, cortical activity was related primarily to movement direction. As the hand approached the target, cortical discharge was tuned more closely to movement amplitude and target location. Their finding is compatible with the idea that the direction of an arm movement is specified fully at the time of movement onset but that the specification of movement extent evolves gradually. Observations of Georgopoulos and Massey (1988) are also consonant with the idea that movement direction is fully specified at the time of movement onset. These observations, in conjunction with the findings we have presented here, suggest the intriguing idea that the specification of different parameters of a movement evolves in parallel but with time courses that can differ substantially.

Our results have negated two hypotheses that we set out to test, namely, that the posture of the hand does not reflect the shape of the object as the hand approaches it and alternatively, that the hand already is molded to the object's shape at the time of maximum hand opening. A third alternative would be that there are a few discrete hand postures, adopted at the time of maximum aperture, for example, a default posture for convex shapes, another one for concave shapes, and a third for flat shapes. If that were so, one would expect a clustering of the points when they are plotted in discriminant space. The results in Figs. 11 and 12, which were typical of the results for all subjects, do not support this hypothesis either. Instead, it appears that in this experiment hand posture was molded along a continuum according to the contours of the object to be grasped.

Finally, we wish to comment on the observation that the matching experiment gave much poorer discrimination of object shapes than did the reaching task. On average, the SME for matching was comparable with the value at 50% of movement duration, but the SD of the postures was about twice as great in the matching task as it was during the movement. Taken together, these results suggest that, on average, the hand postures during the matching task were more distinct from each other than they were at 50% of movement duration but that the greater amount of variability led to a poorer resolution. One factor that could account for this result is that vision of the arm was available during the grasping task but not during the matching task. However, we believe another explanation is more likely. There is growing evidence that the control of the proximal and distal musculature of the arm is not entirely independent (cf. Paulignan and Jeannerod 1996; Soechting and Flanders 1993). Therefore, it seems likely that the matching task, requiring subjects to execute the distal component (hand shape) in the absence of the proximal component (transport) was more difficult to control and therefore associated with a greater amount of variability.

We thank Dr. Martha Flanders for helpful discussions during the course of this project.

This work was supported by National Institute of Neurological Disorders and Stroke Grant NS-15018.

Address for reprint requests: J. F. Soechting, Dept. of Physiology, 6-255 Millard Hall, University of Minnesota, Minneapolis, MN 55455.

Received 9 September 1997; accepted in final form 14 November 1997.

REFERENCES

Bezdek, J. C. *Pattern Recognition with Fuzzy Objective Function Algorithms.* New York: Plenum, 1981.

Chieffi, S. and Gentilucci, M. Coordination between the transport and the grasp components during prehension movements. *Exp. Brain Res.* 94: 471–477, 1993.

Cole, K. J. and Abbs, J. H. Coordination of three-joint digit movements for rapid finger-thumb grasp. *J. Neurophysiol.* 55: 1407–1423, 1986.

Cutkosky, M. R. and Howe, R. D. Human grasp choice and robotic grasp analysis. In: *Dextrous Robot Hands*, edited by S. T. Venkataraman and T. Iberall. New York: Springer, 1990, p. 5–31.

Favilla, M., Gordon, J., Hening, W., and Ghez, C. Trajectory control in targeted force impulses. VII. Independent setting of amplitude and direction in response preparation. *Exp. Brain Res.* 79: 530–538, 1990.

Favilla, M., Hening, W., and Ghez, C. Trajectory control in targeted force impulses. VI. Independent specification of response amplitude and direction. *Exp. Brain Res.* 75: 280–294, 1989.

Fu, Q.-G., Flament, D., Coltz, J. D., and Ebner, T. J. Temporal encoding of movement kinematics in the discharge of primate primary motor and premotor neurons. *J. Neurophysiol.* 73: 836–854, 1995.

Georgopoulos, A. P. and Massey, J. T. Cognitive spatial-motor processes. II. Information transmitted by the direction of two dimensional arm movements and by neuronal populations in primate motor cortex and area 5. *Exp. Brain Res.* 69: 315–326, 1988.

Ghez, C., Favilla, M., Ghilardi, M. F., Gordon, J., Bermejo, R., and Pullman, S. Discrete and continuous planning of hand movements and isometric force trajectories. *Exp. Brain Res.* 115: 217–233, 1997.

Hajian, A. Z. and Howe, R. D. Identification of the mechanical impedance at the human finger tip. *J. Biomech. Eng.* 119: 109–114, 1997.

Iberall, T. and Fagg, A. H. Neural network models for selecting hand shapes. In: *Hand and Brain. The Neurophysiology and Psychology of Hand Movements,* edited by A. M. Wing, P. Haggard, and J. R. Flanagan. San Diego, CA: Academic, 1996, p. 243–264.

Iberall, T. and MacKenzie, C. L. Opposition space and human prehension. In: *Dextrous Robot Hands,* edited by S. T. Venkataraman and T. Iberall. New York: Springer Verlag, 1990, p. 32–54.

Jeannerod, M. Intersegmental coordination during reaching at natural visual objects. In: *Attention and Performance IX,* edited by J. Long and A. Baddeley. Hillsdale: Erlbaum, 1981, p. 153–168.

Jeannerod, M. The timing of natural prehension movements. *J. Mot. Behav.* 16: 235–254, 1984.

JOHANSSON, R. S. AND COLE, K. J. Sensory-motor coordination during grasping and manipulative actions. *Curr. Opin. Neurobiol.* 2: 815–823, 1992.

JOHNSON, K. O. AND PHILLIPS, J. R. Tactile spatial resolution. I. Two-point discrimination, gap detection, grating recognition. *J. Neurophysiol.* 46: 1177–1191, 1981.

JOHNSON, R. A. AND WICHERN, D. W. *Applied Multivariate Statistical Analysis.* Englewood Cliffs, NJ: Prentice Hall, 1992.

MARTENIUK, R. G., MACKENZIE, C. L., AND ATHENES, S. Functional relationships between grasp and transport components in a prehension task. *Hum. Mov. Sci.* 9: 149–176, 1990.

NAPIER, J. R. The prehensile movements of the human hand. *J. Bone Joint Surg.* 38B: 902–913, 1956.

PAULIGNAN, Y. AND JEANNEROD, M. Prehension movements. The visuomotor channels hypothesis revisited. In: *Hand and Brain. The Neurophysiology and Psychology of Hand Movements*, edited by A. M. Wing, P. Haggard, and J. R. Flanagan. San Diego, CA: Academic, 1996, p. 265–282.

PAULIGNAN, Y., JEANNEROD, M., MACKENZIE, C., AND MARTENIUK, R. Selective perturbation of visual input during prehension movements. II. The effects of changing object size. *Exp. Brain Res.* 87: 407–420, 1991.

SAKITT, B. Visual-motor efficiency (VME) and the information transmitted in visual-motor tasks. *Bull. Psych. Soc.* 16: 329–332, 1980.

SANTELLO, M. AND SOECHTING, J. F. Matching object size by controlling finger span and hand shape. *Somatosens. Mot. Res.* 14: 203–212, 1997.

SHANNON, C. E. The mathematical theory of communication. *Bell Syst. Techn. J.* 27: 379–423, 1948.

SOECHTING, J. F. AND FLANDERS, M. Parallel, interdependent channels for location and orientation in sensorimotor transformations for reaching and grasping. *J. Neurophysiol.* 70: 1137–1150, 1993.

SOECHTING, J. F. AND FLANDERS, M. Flexibility and repeatability of finger movements during typing: analysis of multiple degrees of freedom. *J. Comput. Neurosci.* 4: 29–46, 1997.